Structure and Origin of a Small Cyclonic Eddy Observed during the POLYMODE Local Dynamics Experiment*

ERIC J. LINDSTROM**

School of Oceanography WB-10, University of Washington, Seattle, WA 98195

CURTIS C. EBBESMEYER***

Evans-Hamilton, Inc., 6306 21st Avenue N.E., Seattle, WA 98115

W. BRECHNER OWENS

Woods Hole Oceanographic Institution, Woods Hole, MA 02543

(Manuscript received 11 July 1983, in final form 19 April 1984)

ABSTRACT

In the POLYMODE Local Dynamics Experiment (31°N; 69.5°W) a small cyclonic eddy was discovered and mapped. The eddy was characterized by an upward doming of isotherms in the upper part of the main thermocline. The dynamical signal extended from the surface downward to a pressure of 800 db and outwards to a radius of 25–30 km. There was no deep-water property signal associated with the eddy, but a layer (~10 m thick) of very low salinity water was observed at the sea surface immediately above the feature. The salinities in the surface layer were lower than any reported in the historical hydrographic data for the region. Rainfall is discounted as a possible source of this signal because of the layer's thickness and horizontal scale. Alternatively the closest source for the low salinity is in the Slope Water, some 500 km away. The eddy may have originated by the splitting of a Gulf Stream ring, a hypothesis which is supported by observations of eddies of similar size and structure near several Gulf Stream rings. This mechanism could also account for the unusually low surface salinities since rings may trap Slope Water and transport it into the Sargasso Sea.

1. Introduction

One of the interesting results of the POLYMODE Local Dynamics Experiment was the discovery of numerous small eddies with diameters less than 50 km. Because the hydrographic station spacing of the LDE was 25 km, nearly all occurrences of these small eddies were documented on the basis of only one or two stations. These observations are summarized by Lindstrom and Taft (1986) elsewhere in this issue. Two small eddies were intentionally sampled at higher spatial resolution (12.5 km), yielding enough data to warrant individual analyses. Elsewhere in this issue Elliott and Sanford (1986a,b) discuss the subthermocline anticyclonic eddy "D1." This paper examines the observations taken in the second eddy, "S2,"[1] which had a cyclonic circulation extending downwards from the sea surface into the main thermocline. A third small eddy, "S1," with anticyclonic circulation is discussed by Riser et al. (1986) in this volume. This eddy was also discovered during the LDE, but was only sampled extensively outside of the LDE array.

Shallow eddy 2 was discovered on 26 June 1978 during the fourth of the large-scale surveys of the LDE density program. It appeared as an upward doming of the upper main thermocline at a single hydrographic station at the center of the LDE sampling grid. Subsequently, two surveys of S2 were completed before the large-scale flow carried the eddy out of the LDE mapping area. Our analysis is based on these two surveys in addition to the large-scale maps which place the eddy within the context of the mesoscale eddy features of the region. In addition, data from an array of moored velocity and temperature sensors are examined for evidence of the eddy's passage.

Two aspects of the data are analyzed in the context of the historical hydrographic data from the western North Atlantic. Unusually low salinities at the sea surface above the eddy are discussed at some length because they are the most distinctive characteristic of the eddy's water-property signal. They are the lowest sa-

* Contribution No. 1616 from the School of Oceanography, University of Washington, Seattle, Washington and Contribution No. 5008 from the Woods Hole Oceanographic Institution.

** Present address: CSIRO Marine Laboratories, GPO Box 1538, Hobart, Tasmania, 7001, Australia.

*** Also affiliated with the Marine Sciences Research Center, State University of New York at Stony Brook, New York, 11794.

[1] "S2" stands for Shallow eddy 2. Feature "S1" (Shallow eddy 1) is discussed by Riser et al. (1984) and observations of "D1" (Deep eddy 1) are described by Elliott and Sanford (1984a,b).

linities ever found at the sea surface in the LDE area according to the historical hydrographic data. Secondly, other eddies similar in temperature cross-section from the historical data are documented. These analyses suggest that S2 may be the result of the splitting of a Gulf Stream ring.

2. Data

The LDE density program consisted primarily of the following elements: conductivity, temperature, pressure and oxygen (CTD) profiles; expendable bathythermograph (XBT) profiles; and moored current meters. A preliminary summary of results from the LDE has been given by McWilliams et al. (1983). The calibration and many results of the profiling are provided by Shen et al. (1984) and Taft et al. (1984); those from the current meters are given by Owens et al. (1982). The LDE surveys utilized two ships for mapping water properties during a two-month period from mid-May to mid-July 1978. Seven surveys of hydrographic properties were obtained within a 100-km radius of 31°N, 69.5°W (Fig. 1), each taking approximately five days for completion. CTD profiles were used to describe the water properties in the upper 3 km on a nearly uniform 25-km grid in the mapping area. XBT drops were made midway between the CTD stations yielding 12.5-km resolution of the temperature field in the upper 800 m of the water column. Each mapping of the LDE area was termed a Large Scale (LS) survey. The sampling pattern for one such survey is shown in Fig. 2b. CTD station spacing was reduced to 12.5 km for specific, feature-oriented studies con-

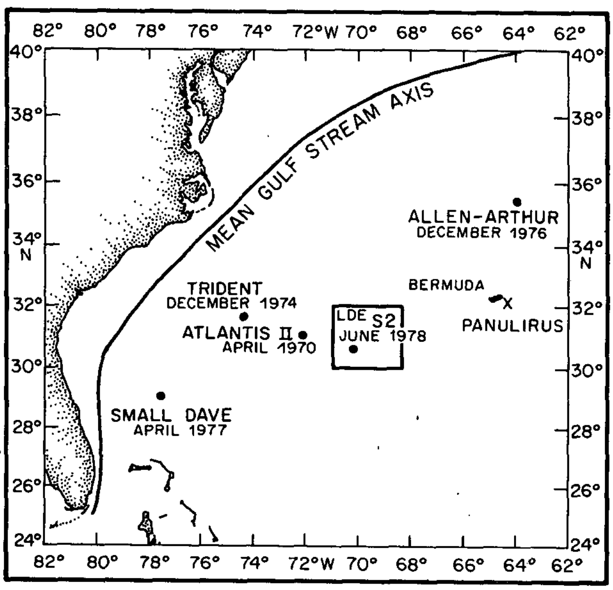

FIG. 1. Locations of the Local Dynamics Experiment (LDE), the eddy S2, and the *Panulirus* hydrographic station (×). Also shown are the locations of several small eddies (dots) having temperature structures similar to S2.

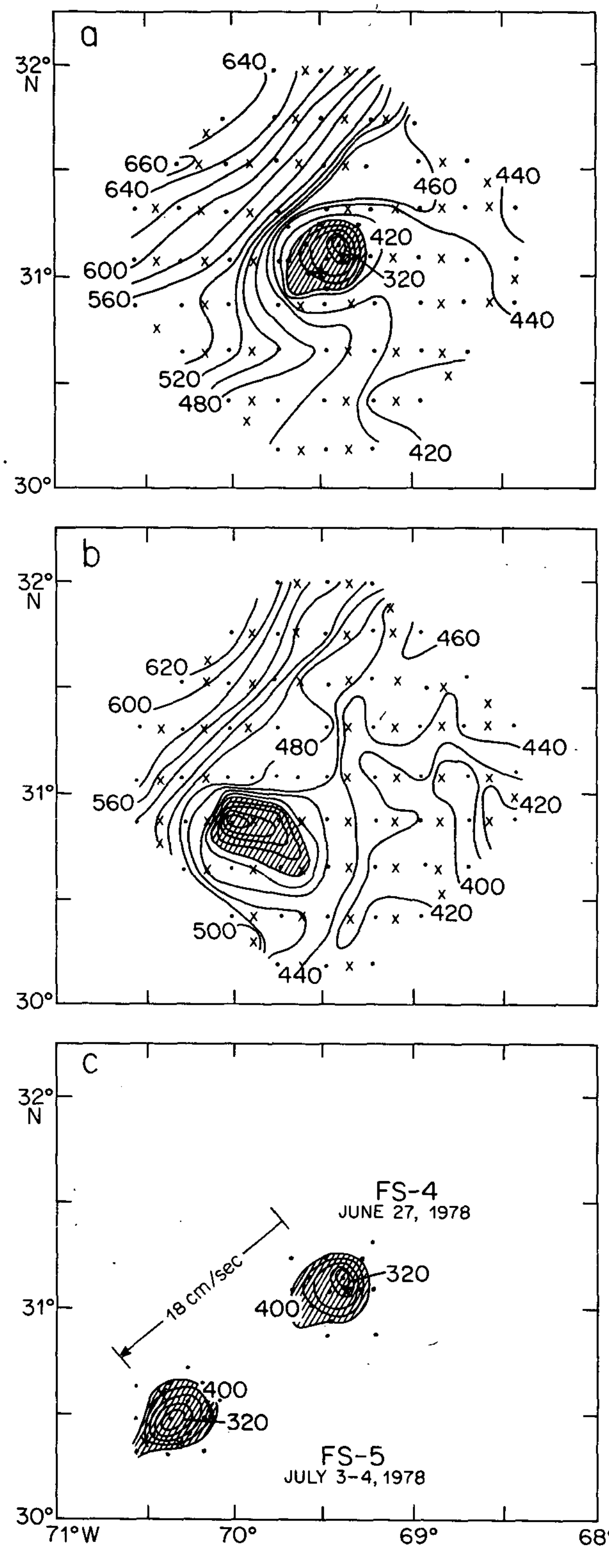

FIG. 2. Maps of 17°C isotherm pressure (db) for the surveys in which eddy S2 was observed: (a) LS-4, 21–26 June 1978; (b) LS-5, 28 June–3 July 1978; (c) FS-4, 27 June 1978 and FS-5, 3–4 July. Notation: ×, XBT station; ●, CTD station; and +, current meter mooring.

ducted after the completion of some LS surveys. These higher resolution mappings were termed Fine Scale (FS) surveys.

The small cyclonic eddy S2 was discovered at the center of the mapping grid at the completion of LS-4 (22–27 June). It was not seen entering the mapping area because of the 10-day gap between LS-3 and LS-4 caused by the mid-experiment port call in Bermuda. Subsequently, the eddy was mapped during FS-4 on June 27th. During LS-5, on the evening of 30 June, S2 was seen in two CTD profiles to the southwest of its previous position. After completing LS-5, we proceeded southwestward and found the eddy at the edge of the mapping area. FS-5 was carried out in the region immediately southwest of the LS grid. By the time of LS-6, S2 presumably moved considerably farther to the southwest, well outside of the fixed mapping area.

As S2 passed through the center of the LDE mapping area, its signal was recorded by velocity and temperature sensors on a mooring. The mooring, at 31.023°N, 69.498°W, had Vector Averaging Current Meters (VACMs) in and above the main thermocline at nominal depths of 269, 394, 516, 616, 715 and 839 m. Each instrument measured in situ temperature as well as velocity over a 15-minute averaging interval, except at a depth of 269 m where the temperature circuit failed. Instruments at depths in excess of 839 m showed no signal associated with S2 and have been omitted from this presentation.

3. Results

a. The hydrographic field

Figure 2a shows a map of 17°C isotherm pressure obtained by combining the data from LS-4 and FS-4; S2 is the low-pressure area near the center of the map. This isotherm was chosen because the maximum upward doming of isotherms associated with the eddy occurs at this temperature. The amplitude of the 17°C isotherm deflection at the eddy center was approximately 130 db when compared to pressures to the southeast where the isotherm relief is smallest. To the northwest, S2 is bordered by a steep deepening of the 17°C isotherm. This deepening is the shallower expression of a gradient which exists throughout the main thermocline.

A better depiction of S2's relationship to this gradient is seen by looking at the zonal temperature section across the center of LS-4 (Fig. 3a). Eastward of the eddy, the thermocline also tends toward slightly greater pressures, suggesting that S2 is centered within a region of large-scale cyclonic shear. The localized upward doming of isotherms in S2 does not extend into the lower thermocline. There, near 5°–6°C, the larger-scale cyclonic shear is suggested by the slight doming of isotherms toward the center of the section. At temperatures less than 3°C, only an east–west gradient in isotherm depth can be seen.

The movement of the eddy to the southwest is evident in Fig. 2b. Here only data from LS-5 are used to contour the map but, because of the coarse sampling of the survey, the details of the eddy core are not well resolved. In the southwest corner of Fig. 2c, S2 is depicted from FS-5 measurements, the last one taken in the eddy. FS-4, as depicted in Fig. 2a, is also shown in Fig. 2c. The pressure pattern of isotherms moved to the southwest at an average speed of 18 cm s^{-1}; a comparison of the temperature structure in the two surveys shows that there is no apparent evolution of the eddy amplitude or shape during the translation.

Zonal sections of temperature, salinity and potential density from LS-4 are shown in Fig. 3. They show the upward doming of the property fields associated with the cyclonic circulation. The deflections of the salinity and oxygen fields below the surface layer are such that the mean LDE T–S and T–O_2 relationships are preserved within the eddy. For brevity the oxygen section, being quite similar to salinity, has been omitted. Figure 4 shows the T–S and T–O_2 relationships for all the fine-scale-survey stations and the ±2 standard deviation envelope of all LDE data. Almost all of the salinity measurements at lower temperatures fall within the envelope. At temperatures greater than 24°C very low salinities are found above the eddy, within about 10 db of the sea surface. The tendency toward low salinities continues downward through the seasonal thermocline to the 18°C water. Several points at 20°C, near the bottom of the seasonal thermocline, also lie outside the two standard deviation envelope. Those few points falling outside the envelope below 18°C are believed to represent natural statistical variability and are not discussed further in connection with the eddy. The oxygen measurements indicate numerous anomalously high values near the bottom of the seasonal thermocline and in the 18°C water. The few points lying outside the envelope between 10° and 16°C occur at a single FS-4 station distant from the eddy core and are also attributed to unrelated variability in the property field.

b. The velocity field

When S2 was first observed on 26 June the central mooring of the current-meter array was within the eddy. From the hydrographic data it was determined that the characteristic isotherm pattern of the eddy was traveling at a speed of 18 cm s^{-1} toward 230°T. Because the eddy was strongly surface-intensified, moved at a high speed, and had a small horizontal scale (less than 50 km in diameter), its signal was suppressed in the analysis of Owens et al. (1982) in which the low-passed velocities at 600 m depth were examined. In order to see the S2 signal it was necessary to reduce the time-averaging to a one-hour running box-car filter with hourly subsampling. The resulting time series for temperature and velocity at several depths, embracing the period when the eddy passed through the mooring, are

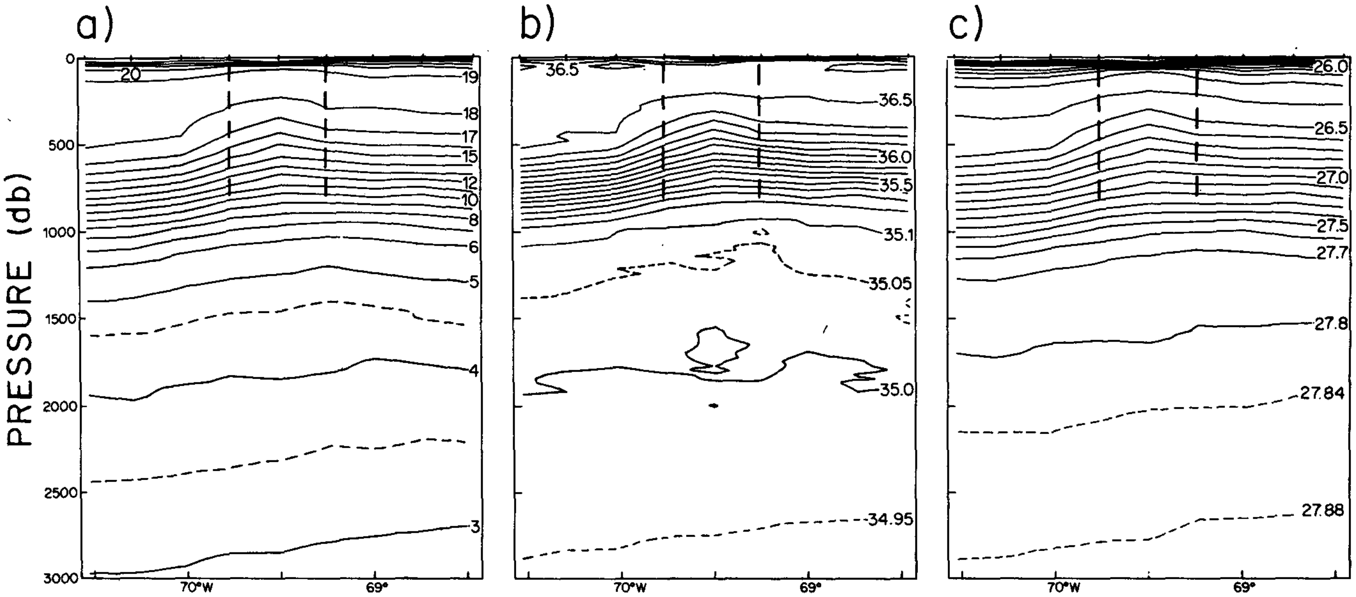

FIG. 3. Zonal sections at 31°N of (a) temperature (°C); (b) salinity (‰) and (c) potential density (kg m^{-3}) from LDE large-scale survey 4. Vertical dashed lines bracket the eddy S2.

shown in Figs. 5 and 6, respectively. It is worth noting that, although the mooring was "blown over" about 20 m during the passage of the eddy, it was unnecessary to apply a pressure correction to the data. If one takes a mean vertical temperature gradient at 400 m of 0.6°C/100 m, then the 20-m deflection results in only a 0.12°C signal due to mooring motion, which is the magnitude of the small-scale perturbations in the temperature time series.

In Fig. 5 the temperature scale for each plot has been chosen to be inversely proportional to the LDE mean vertical temperature gradient. As a result, the displacements shown are proportional to the vertical isotherm displacements, provided the displacements are not too

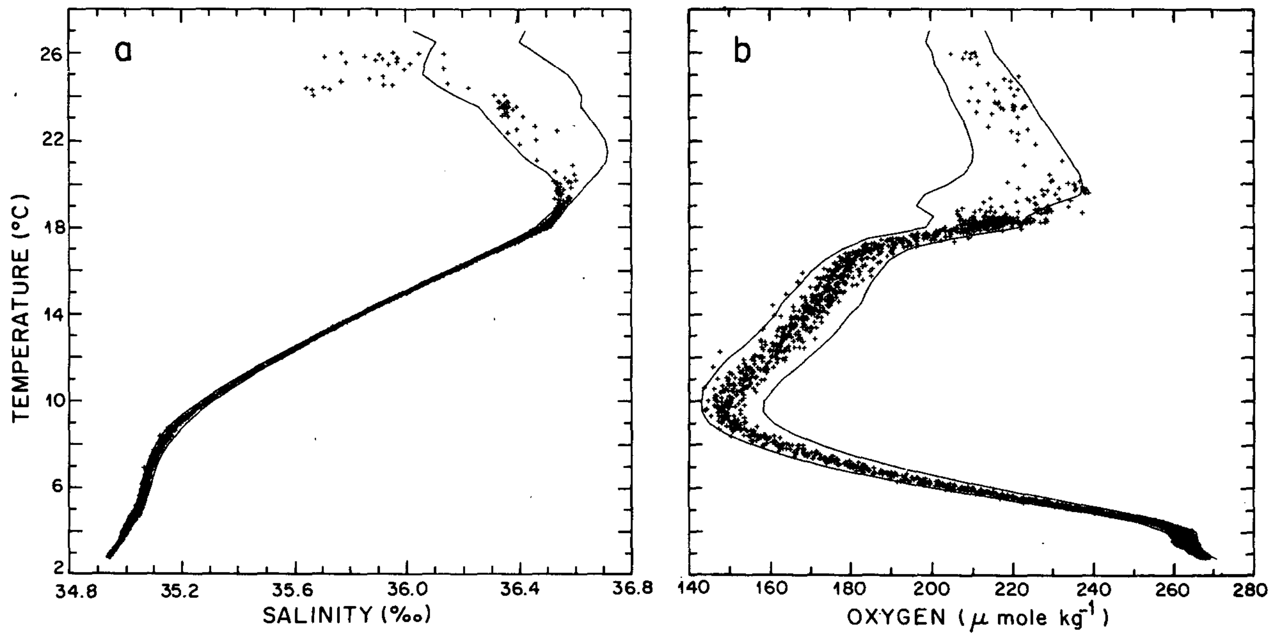

FIG. 4. Temperature–salinity (a) and temperature–oxygen (b) relationships for all the stations taken in the two fine-scale surveys of the eddy. Solid lines embrace ±2 standard deviations of all LDE measurements.

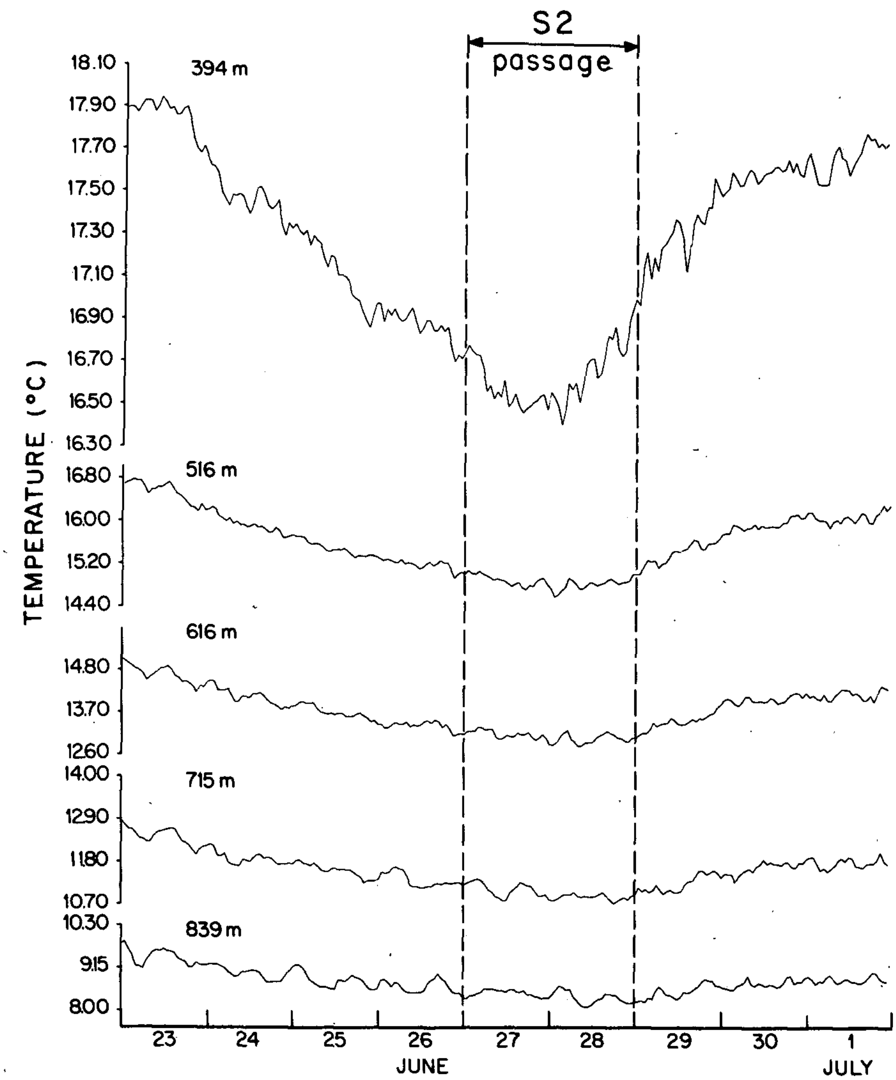

FIG. 5. Temperature versus time at selected depths for five sensors located on the mooring through which the eddy passed. The temperature scale is inversely proportional to the mean vertical temperature gradient. The dashed lines denote the time of S2's passage.

large. For all but the shallowest (394 m) depth this appears to be a good assumption. Nevertheless, the time series of temperature are consistent with the horizontal section of temperature in Fig. 3, as well as the translation speed of 18 cm s^{-1} determined from the CTD surveys. The isotherm doming, present from 23 to 29 June at the mooring, would have a horizontal scale of 90 km (18 cm $s^{-1} \times 0.86$ km d^{-1}/cm $s^{-1} \times 6$ d), which is comparable to that of the larger-scale isotherm pattern (Fig. 3). The signature of S2 appears as a sharp temperature decrease at 394 m from 27 through 29 June (vertical dashed lines in Fig. 5). This signal decays rapidly in the vertical such that there is a much reduced signal at 516 and 616 m and no obvious signal at 715 m.

The time series of temperature and the hydrographic maps demonstrate clearly that S2 is coupled with a larger-scale shear flow which cannot be modeled as a simple, uniform flow for several reasons. The small eddy is located near the center of a horizontal cyclonic shear which has a horizontal scale only 2 to 3 times larger than S2. As a result there are significant gradients of the larger-scale flow in the vicinity of S2. Thus, any velocity structure which one attributes to the small-scale eddy will depend crucially on the attributes of the large-scale flow. This is in strong contrast to the two other well-documented small-scale eddies seen in the LDE (Elliott and Sanford, 1984a,b; Riser et al., 1984), where the large-scale flow could be approximated by a uniform flow which passively advected the small eddies.

The velocity time series for the six instruments in and above the main thermocline shown in Fig. 6 demonstrate the coupled structure of S2 and the larger-

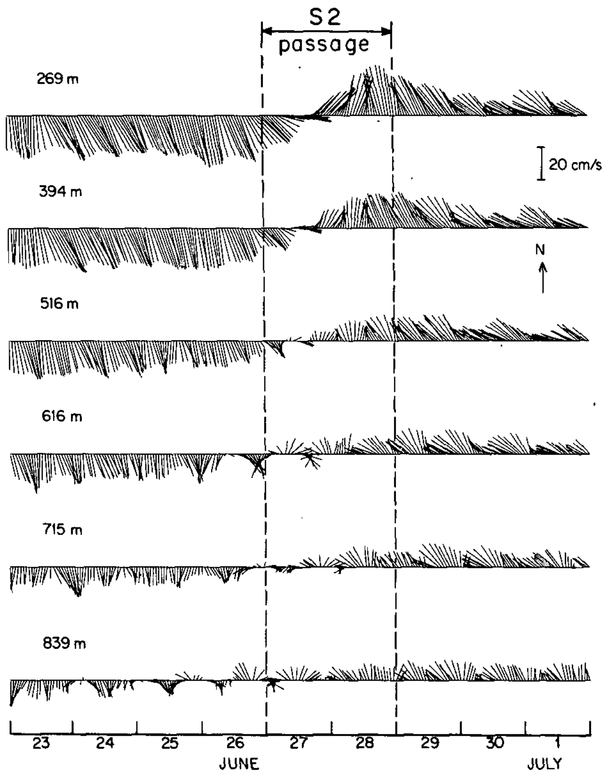

FIG. 6. Time series of velocity vectors at selected depths from the mooring through which S2 passed. The dashed lines denote the time of S2's passage.

scale flow. The interval when S2 passed the mooring is once again highlighted within vertical dashed lines. As was the case for the temperature time series, it is evident that S2 is embedded in a background baroclinic flow which has horizontal and temporal scales that are not much larger than its own. In addition, the velocity is not in the direction of S2's translation either before or after the passage of the eddy. From the horizontal structure of the low-passed velocities at 600 m depth from the LDE current meter array (Owens et al., 1982), it appears that this larger-scale flow is a mesoscale eddy which is propagating with a speed and direction similar to that estimated for S2. Given the complex structure, it cannot be determined whether S2 is being passively advected or if there is some component of self-propagation.

Although the horizontal structure of S2's velocity field cannot be determined, the vertical extent of the velocity signal can still be seen in Fig. 6. On 28 June the enhanced northward velocities seen at the upper two current meters (294 and 394 m) are due to S2. At 516 m depth the signal is much reduced and at 616 m it cannot be detected in the time series. The signal for the first half of the S2's passage by the mooring is not obvious in the time series because of the presence of the larger-scale circulation. From the velocity structure on 28 June, it appears that S2 has a velocity signal of 10–15 cm s^{-1} at 269 m depth and vertical decay scale similar to that indicated by the temperature time series.

4. Discussion

Because the low-salinity water near the sea surface is the strongest water property anomaly associated with S2 and may give a clue to its origin, a close examination of this signal is warranted. Figure 7 shows maps of the salinity averaged over the upper 10 db of the water column for the S2 surveys. On each map very low salinities (35.7‰) are found over the eddy core, as located by the 17°C isotherm topography in Fig. 2. The spatial scale of the anomalous water (<36.1‰) is about 50–75 km. Substantial distortion of the surface isohalines is seen at the periphery of the eddy, but the core of low-salinity water appears to be trapped over the eddy during these observations. It may be that the comparatively fresh water is the result of precipitation and has not been associated with the eddy's thermocline structure since its origin. On the other hand, if the surface water has been trapped by the dynamical structure of S2 since its formation we must locate the source for such water and provide a plausible mechanism for the generation of the dynamical structure at that location.

The low surface salinity is put in some perspective by comparing it with a subsample of the historical data of Ebbesmeyer and Taft (1979) compiled for the LDE area. In the 4° square centered on the LDE, the historical record of surface salinity for June and July contains only one observation below 36.1‰ as shown by a histogram of surface salinity values (Fig. 8). A mean salinity close to 36.4‰ is expected in this area; the water above S2 is about 0.7‰ below this mean. The histogram of surface salinities from the *Panulirus* site (32.18°N; 64.50°W), where hydrographic data have been taken once or twice monthly for nearly a quarter century, is also shown in Fig. 8. Both histograms show that the salinities above S2 are lower than previously observed in the central Sargasso Sea.

The amount of rainfall needed to reduce the salinity of the top 10 db to values observed over the eddy is about 15–20 cm. The mean precipitation for the entire June–August period in the LDE area is about 30 cm (Dorman and Bourke, 1981). This suggests that an unusually strong and persistent precipitation event would be required to account for the observed anomaly. No such events were observed during the LDE fieldwork. A subsequent search of large-scale 6-hourly surface meteorological charts did not indicate major frontal activity which might have led to a significant rainfall event in the LDE area.

Other evidence that weighs against the precipitation hypothesis is the horizontal scale (50–75 km) of the salinity anomaly (defined by the 36.1‰ contour). This scale is about an order of magnitude larger than precipitation signatures in the Sargasso Sea surface layer studied by Ginzburg et al. (1980). In that study, patches

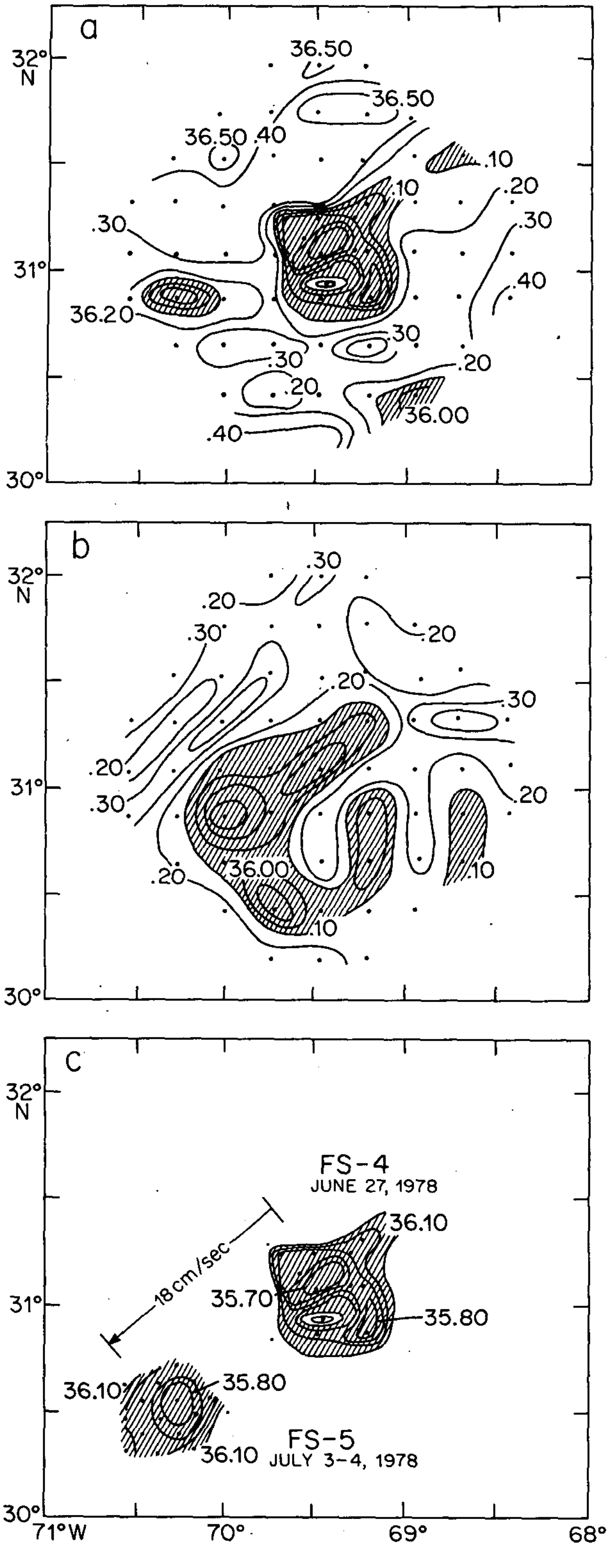

FIG. 7. Maps of the mean salinity (‰) in the upper 10 db for surveys in which the eddy S2 was observed: (a) LS-4, 21–26 June 1978; (b) LS-5, 28 June–3 July 1978; (c) FS-4, 27 June 1978 and FS-5, 3–4 July 1978. Hatched areas have salinities less than 36.1‰. In (c) the advection speed of S2 is shown as 18 cm s^{-1}.

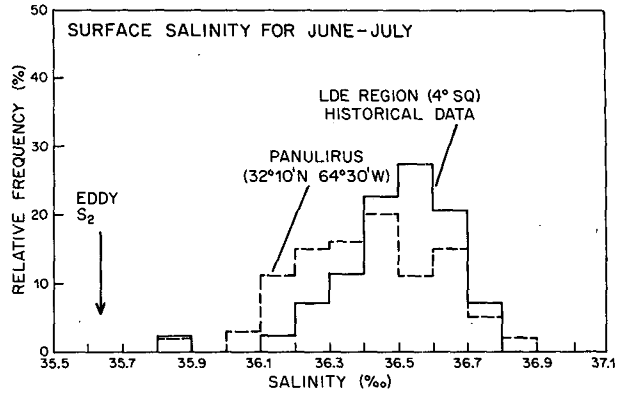

FIG. 8. Histograms of sea surface salinity during June and July from the historical hydrographic data in the 4° square centered on the LDE (solid, 44 observations), and from the 20-year time series of hydrographic measurements made at the *Panulirus* hydrographic station (dashed, 92 observations; see Fig. 1 for location).

of rainfall-induced, low-salinity water were 4–8 km in size. This patch size was thought to correspond to the sizes of the cumulonimbus clouds that produced the precipitation. Farther south in the Atlantic Ocean, Elliott (1974) studied the effects of rainfall during the Barbados Oceanographic and Meteorological Experiment (17.5°N; 54.5°W). He found that a less dense, stably stratified layer did not persist in response to precipitation, but rather, a fluctuating salinity profile was observed at times of heavy rain.

The foregoing evidence indicates that rainfall was not the source of the low-salinity water above S2; as a result, other hypotheses involving horizontal advective processes and distant sources were examined for the origin of the near-surface water. The likely sources of such low-salinity surface water are landward of the Gulf Stream in the Slope Water. The salinities of the Slope Water at the sea surface are about 35.5‰ as shown in the *T–S* relationship for those waters shown in Fig. 9. A warming of this water type by 4°C would bring the water to the *T–S* characteristics observed over S2. The mean monthly sea surface temperature (SST) maps for the western North Atlantic compiled by Schroeder (1966) show an average increase in SST of 2°C per month during late spring and early summer for the central Sargasso Sea. This suggests that the modification of Slope Water by 4°C would take approximately two months.

It seems reasonable to assume that some protecting dynamical structure would be necessary in order to transport surface waters, without significant dilution, from north of the Gulf Stream hundreds of kilometers southward to the LDE area. The near-surface waters of Gulf Stream rings have been observed to maintain low salinity for periods of months after formation (Fuglister, 1977). The sea surface temperature signal may be changed or eliminated by heating, but the surface salinity signal of rings is more persistent (The Ring

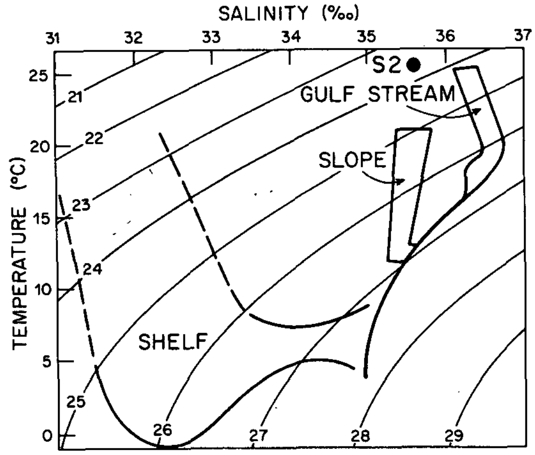

FIG. 9. Temperature–salinity relationship for Gulf Stream, Slope, Shelf waters (adapted from Ford et al., 1952), and those observed at the sea surface above the S2. Isopleths of constant σ_t are superimposed on the diagram.

Group, 1981). The fact that S2 should have a near-surface water property signal and no corresponding deeper signal is quite intriguing. If it were itself a ring (albeit a small one), we might reason that it is relatively young because it has a significant surface salinity signal, yet neither its amplitude nor its deeper water properties suggest this youth (cf. young rings as described by The Ring Group, 1981).

An alternative hypothesis, which would account for S2's small size, is that the eddy is the result of the splitting of a Gulf Stream ring. The shedding of a cyclonic eddy by a ring has been explored theoretically by Ikeda (1981). He found that larger rings are unstable to asymmetric disturbances and split after being elongated along one axis.

Ring instability may have been observed by Cheney et al. (1976). While surveying a Gulf Stream ring near 32°N, 73°W in December 1974, they observed the elongation of a nearly circular ring and the eventual spawning of a separate small cyclonic eddy. An XBT section through this small feature is shown in Fig. 10c. Its size, shape and vertical structure are similar to that of S2, whose vertical temperature section from FS-5 is shown in Fig. 10a. The section through this eddy was made before its complete separation from its parent ring so that it blends into the ring to the east, accounting for its small apparent amplitude. We refer the reader to Cheney et al. (1976) for plan views of the isotherm pressures showing the evolution of the splitting event.

A small eddy quite similar in structure to S2 was observed near 29°N, 77°W in April 1977. An XBT section through this feature is shown in Fig. 10d. This eddy was observed to the east of Gulf Stream ring "Dave" discussed by Richardson (1980). The separation of the smaller eddy, "Small Dave", from its larger companion is distinctly shown in the track of a free drifting buoy launched at the time of observation. The trajectory, shown by Richardson et al. (1979a), indicates that the buoy made cyclonic loops in a small eddy before escaping and subsequently being entrained in the structure of ring Dave. We speculate that Small Dave may be the result of yet another ring-splitting event involving the larger ring Dave.

Ring splitting, resulting in a small cyclonic eddy, also was observed in late 1976 and early 1977 closer to the Gulf Stream in the case of rings Allen and Arthur. This event is discussed by Richardson et al. (1979b). The eddies were judged to have diameters of 165 km for Allen and 65 km for Arthur, just before the time of their complete separation.

These three cases indicate that a small cyclonic eddy of S2's size may be produced in the process of Gulf Stream ring decay by splitting. Although no other examples of S2-type features related to ring splitting were found, another small cyclonic eddy observed in the vicinity of the LDE site looked very much like S2. The feature was discussed by Barrett (1971) and was observed in April 1970 near 31°N, 72°W. An XBT section through this eddy is shown in Fig. 10b; it shows the dome-like structure of the upper-thermocline isotherms and the absence of an identifiable thermal structure in the near-surface layer. No significant water mass differences between the water within and outside of the eddy were observed.

Given these examples the most attractive explanation of the LDE observations is that the eddy is the result of a ring-splitting event.

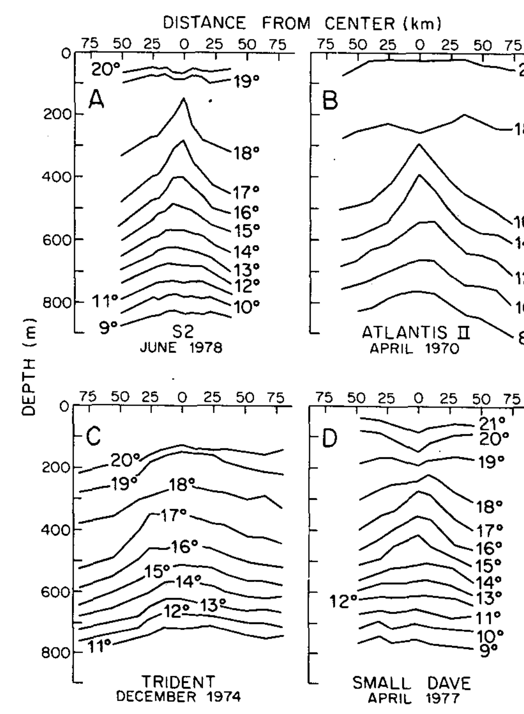

FIG. 10. Temperature (°C) sections through eddy S2 and three similarly shaped eddies (b, c and d; for locations see Fig. 1).

5. Conclusion

Both the low surface salinity and the geometry of isotherm patterns in the small eddy S2 provided us with plausible explanations as to its origin. That Slope Water existed over the eddy core, as well as the similarity in structure to small cyclonic eddies originating from Gulf Stream rings, led us to speculate that S2 was the product of a ring-splitting event. The proposed ring splitting was not observed and no Gulf Stream ring was observed in the LDE locality, thus we base our proposed origin only on the circumstantial evidence presented here.

This work suggests that further theoretical study of ring instability would be useful. Observationally, time scales for ring splitting may dictate more frequent sampling of large rings than has previously been attempted. Constant weekly sampling would be required to observe the splitting process. It is possible that ring splitting is common but has gone unnoticed because of infrequent and sporadic sampling of Gulf Stream rings. Lifetimes of the spawned eddies are unknown; observation of these features over an extended period of time would be interesting, both in terms of their decay and movement.

Acknowledgments. This work was funded by the National Science Foundation in grants to the University of Washington (OCE 79-23951 and OCE 80-24912) and to the Woods Hole Oceanographic Institution (OCE 77-19403 and OCE 82-00154). We thank Philip L. Richardson, William J. Jenkins and the staff of the National Oceanographic Data Center for providing us with data. We also thank James C. McWilliams, Charles E. Parker, Bruce A. Taft and Colin Y. Shen for the many helpful comments they made during discussions of this work and Jackie Firth of the CSIRO Marine Laboratories for typing the final manuscript.

REFERENCES

Barrett, J. R., 1971: Available potential energy of Gulf Stream rings. *Deep-Sea Res.*, **18,** 1221–1231.

Cheney, R. E., W. H. Gemmill, M. K. Shank, P. L. Richardson and D. Webb, 1976: Tracking a Gulf Stream ring with SOFAR floats. *J. Phys. Oceanogr.*, **6,** 741–749.

Dorman, C. E., and R. H. Bourke, 1981: Precipitation over the Atlantic Ocean, 30°S–70°N. *Mon. Wea. Rev.*, **109,** 554–563.

Ebbesmeyer, C. C., and B. A. Taft, 1979: Variability of potential energy, dynamic height and salinity in the main pycnocline of the western North Atlantic. *J. Phys. Oceanogr.*, **9,** 1073–1089.

Elliott, B. A., and T. B. Sanford, 1986a: The subthermocline lens D1. Part I: Description of its water properties and velocity profiles. *J. Phys. Oceanogr.*, **16,** 532–548.

——, and ——, 1986b: The subthermocline lens D1. Part II: Kinematics and dynamics. *J. Phys. Oceanogr.*, **16,** 549–561.

Elliott, G. W., 1974: Precipitation signatures in the sea-surface-layer conditions during BOMEX. *J. Phys. Oceanogr.*, **4,** 498–501.

Ford, W. L., J. R. Longard and R. E. Banks, 1952: On the nature, occurrence and origin of cold low salinity water along the edge of the Gulf Stream. *J. Mar. Res.*, **11,** 281–293.

Fuglister, F. C., 1977: A cyclonic ring formed by the Gulf Stream, 1967. *A Voyage of Discovery,* M. V. Angel, Ed., Pergamon, 177–198.

Ginzburg, A. I., A. G. Zatsepin, V. Ye. Sklyarov and K. N. Fedorov, 1980: Precipitation effects in the near-surface layer of the ocean. *Oceanology,* **20,** 544–549.

Ikeda, M., 1981: Instability and splitting of mesoscale rings using a two-layer quasigeostrophic model on an F-plane. *J. Phys. Oceanogr.*, **11,** 987–998.

Lindstrom, E. J., and B. A. Taft, 1984: Small water-property transporting eddies: Statistical outliers in the hydrographic data of the POLYMODE Local Dynamics Experiment. *J. Phys. Oceanogr.*, **16,** 613–631.

McWilliams, J. C., and the LDE group, 1983: The local dynamics of eddies in the western North Atlantic. *Eddies in Marine Science,* A. R. Robinson, Ed., Springer-Verlag.

Owens, W. B., J. R. Luyten and H. Bryden, 1982: Moored velocity measurements during the POLYMODE Local Dynamics Experiment. *J. Mar. Res.*, **40**(Suppl.), 509–524.

Richardson, P. L., 1980: Gulf Stream ring trajectories. *J. Phys. Oceanogr.*, **10,** 90–104.

——, J. J. Wheat and D. Bennett, 1979a: Free-drifting buoy trajectories in the Gulf Stream system. WHOI Tech. Rep. 79-4.

——, C. Maillard and T. B. Sanford, 1979b: The physical structure of life history of cyclonic Gulf Stream ring Allen. *J. Geophys. Res.*, **84,** 7727–7741.

Riser, S. D., W. B. Owens, H. T. Rossby and C. C. Ebbesmeyer, 1986: The structure, dynamics, and origin of a small-scale lens of water observed in the western North Atlantic thermocline. *J. Phys. Oceanogr.*, **16,** 572–590.

Schroeder, E. H., 1966: Average surface temperatures in the western North Atlantic. *Bull. Mar. Sci.*, **16,** 302–323.

Shen, C. Y., J. C. McWilliams, B. A. Taft, C. C. Ebbesmeyer and E. J. Lindstrom, 1984: The mesoscale spatial structure and evolution of dynamical and scalar properties observed in the northwestern Atlantic Ocean during the POLYMODE Local Dynamics Experiment. *J. Phys. Oceanogr.*, **16,** 454–482.

Taft, B. A., E. J. Lindstrom, C. C. Ebbesmeyer, C. Y. Shen and J. C. McWilliams, 1984: Water mass structure during the POLYMODE Local Dynamics Experiment. *J. Phys. Oceanogr.*, **16,** 403–426.

The Ring Group, 1981: Gulf Stream cold-core rings: Their physics, chemistry and biology. *Science,* **212,** 1091–1100.